



**HAL**  
open science

## Subfunctionalization of arylalkylamine N-acetyltransferases in the sea bass *Dicentrarchus labrax*: two-ones for one two

Charles-Hubert Paulin, Damien Cazaméa-Catalan, Bina Zilberman-Peled,  
Patricia Herrera-Perez, Sandrine Sauzet, Elodie Magnanou, Michael Fuentès,  
Yoav Gothilf, Jose Antonio Muñoz-Cueto, Jack Falcón, et al.

### ► To cite this version:

Charles-Hubert Paulin, Damien Cazaméa-Catalan, Bina Zilberman-Peled, Patricia Herrera-Perez, Sandrine Sauzet, et al.. Subfunctionalization of arylalkylamine N-acetyltransferases in the sea bass *Dicentrarchus labrax*: two-ones for one two. *Journal of Pineal Research*, 2015, 59 (3), pp.354-364. 10.1111/jpi.12266 . hal-01204652

**HAL Id: hal-01204652**

**<https://hal.sorbonne-universite.fr/hal-01204652>**

Submitted on 24 Sep 2015

**HAL** is a multi-disciplinary open access archive for the deposit and dissemination of scientific research documents, whether they are published or not. The documents may come from teaching and research institutions in France or abroad, or from public or private research centers.

L'archive ouverte pluridisciplinaire **HAL**, est destinée au dépôt et à la diffusion de documents scientifiques de niveau recherche, publiés ou non, émanant des établissements d'enseignement et de recherche français ou étrangers, des laboratoires publics ou privés.

**Sub-functionalization of arylalkylamine *N*-acetyltransferases in  
the sea bass *Dicentrarchus labrax*: Two ones for one two**

PAULIN Charles-Hubert<sup>1</sup>, CAZAMEA-CATALAN Damien<sup>1</sup>, ZILBERMAN-PELED Bina<sup>3</sup>, HERRERA-  
PEREZ Patricia<sup>2</sup>, SAUZET Sandrine<sup>1\*</sup>, MAGNANOU Elodie<sup>1</sup>, FUENTÈS Michael<sup>1</sup>, GOTHILF  
Yoav<sup>3</sup>, MUÑOZ-CUETO Jose Antonio<sup>2</sup>, FALCON Jack<sup>1</sup>, BESSEAU Laurence<sup>1</sup>

<sup>1</sup>Sorbonne Universités, UPMC Univ Paris 06, CNRS, Biologie Intégrative des Organismes  
Marins (BIOM), Observatoire Océanologique, F-66650, Banyuls/Mer, France

<sup>2</sup>Departamento de Biología, Facultad de Ciencias del Mar y Ambientales, Universidad de  
Cádiz. Campus de Excelencia Internacional del Mar (CEI-MAR). Polígono Rio San Pedro,  
11510 Puerto Real, Cádiz, Spain

<sup>3</sup>University of Tel Aviv, Department of Neurobiology, George S. Wise Faculty of Life Sciences  
and Sagol School of Neurosciences, Tel Aviv, Israel

**\*Current address:** CNRS et Université Claude Bernard Lyon 1, UMR 5558, Laboratoire de  
Biométrie et Biologie Evolutive, 43 boulevard du 11 Novembre 1918, F-69622 Villeurbanne  
Cedex, France

**Corresponding author:** Jack Falcón, Laboratoire Aragó, UMR7232, Biologie Intégrative des  
Organismes Marins (BIOM), Observatoire Océanologique, Avenue du Fontaulé, F-66650,  
Banyuls sur Mer, France.

Phone: +33/0 468 88 73 92; FAX: +33/0 468 88 73 98; e-mail: [falcon@obs-banyuls.fr](mailto:falcon@obs-banyuls.fr)

**Running title:** Sea bass arylalkylamine *N*-acetyltransferases

**Key words:** Arylalkylamine *N*-acetyltransferase, Dopamine, Serotonin, Melatonin, Retina,  
Pineal Organ, Teleost Fish

## ABSTRACT

Melatonin is an important component of the vertebrates circadian system, synthesized from serotonin by the successive action of the arylalkylamine *N*-acetyltransferase (Aanat: serotonin→*N*-acetylserotonin) and acetylserotonin-*O*-methyltransferase (Asmt: *N*-acetylserotonin→melatonin). Aanat is responsible for the daily rhythm in melatonin production. Teleost fish are unique because they express two Aanat genes, *aanat1* and *aanat2*, mainly expressed in the retina and pineal gland, respectively. *In silico* analysis indicated that the teleost specific whole genome duplication generated Aanat1 duplicates (*aanat1a* and *aanat1b*); some fish express both of them, while others express either one of the isoforms. Here we bring the first information on the structure, function and distribution of Aanat1a and Aanat1b in a teleost, the sea bass *Dicentrarchus labrax*. Aanat1a and Aanat1b displayed a wide and distinct distribution in the nervous system and peripheral tissues, while *Aanat2* appeared as a pineal enzyme. Co-expression of Aanats with *asmt* was found in the pineal gland and the three retinal nuclear layers. Enzyme kinetics indicated subtle differences in the affinity and catalytic efficiency of Aanat1a and Aanat1b for indole- and phenyl-ethylamines respectively. Our data are consistent with the idea that Aanat2 is a pineal enzyme involved in melatonin production, while Aanat1 enzymes have a broader range of functions including melatonin synthesis in the retina, and catabolism of serotonin and dopamine in the retina and other tissues. The data are discussed in light of the recently uncovered roles of *N*-acetylserotonin and *N*-acetyldopamine as antioxidants, neuroprotectants, and modulators of cell proliferation and enzyme activities.

## INTRODUCTION

Melatonin is an important component of the vertebrates' circadian system. Pineal-derived melatonin controls the daily rhythm in circulating melatonin and provides a hormonal signal of nighttime to the organism. This time-keeping signal controls a number of daily and annual biological rhythms [1]. Retinal melatonin is also produced rhythmically but it acts in an autocrine/paracrine manner [2]. The arylalkylamine *N*-acetyltransferase (Aanat; EC 2.3.1.87), the penultimate enzyme in the melatonin biosynthesis pathway (serotonin → *N*-acetylserotonin), is responsible for the daily rhythm in melatonin production and is, accordingly, named the "timezyme" [3]. The last enzyme in the melatonin biosynthesis pathway, the acetylserotonin-*O*-methyltransferase (Asmt; EC 2.1.1.4: *N*-acetylserotonin → melatonin), displays no apparent daily variation in activity [4, 5] but may contribute, together with Anaat, to the seasonal variations in the melatonin secretion rhythm [6, 7].

Teleost fish are unique among vertebrates because they express two Anaat genes, *aanat1* and *aanat2* [7], as a result of a whole genome duplication [8]. Anaat1 is preferentially expressed in the fish retina and is homologous to the Anaat found in Tetrapods, whereas Anaat2 is preferentially expressed in the fish pineal gland; it has been lost in other vertebrates [9]. Anaat1 and Anaat2 display different kinetics and mechanisms of regulation [2]. Pineal Anaat2 has high affinity for indolethylamines, exhibits a species-specific temperature dependency and always follows a nocturnal activity pattern [9, 10]. In contrast, retinal Anaat1 has affinity for both indoleamines and phenylethylamines, and a similar response to temperature in all the species investigated so far. In addition, Anaat1 may increase either at night or during day, or display no rhythmic pattern at all, depending on the species investigated or, within the same species, on the time of the year [2, 11]. This picture has been enriched by the results of an *in silico* analysis of the available Anaat sequences,

which led to the conclusion that two *aanat1* genes, *aanat1a* and *aanat1b*, are expressed in some distant Teleost [8, 12]. This received the first experimental support after *aanat1a* and *aanat1b* had been cloned from the retina of the sole, *Solea senegalensis* [13]. The two enzymes displayed different expression patterns during metamorphosis: the *1a* isoform was predominant before metamorphosis and did not exhibit rhythmic expression pattern, whereas the *1b* isoform was predominant after metamorphosis and displayed a daily rhythmic pattern in the retina. Analyses of the distribution of Aanat1 and Aanat1b among teleost fish indicated that the split to 1a and 1b isoforms resulted from the teleost specific whole genome duplication (WGD) that occurred at the root of the teleost tree [8]. And, the reason why some fish express both isoforms while others express either one or the other is unclear.

Thus the questions of the evolutionary advantage for some fish to keep the two isoforms and the gain of function of each isoform remain unanswered. Except for the study in the sole that shows a distinct expression pattern of *aanat1a* vs. *aanat1b* at early stages of development [13] virtually nothing is known on the distribution and function of these enzymes in teleost fish. Here we report the cloning of *aanat1a*, *aanat1b*, *aanat2* and *asmt* in a teleost, the sea bass, *Dicentrarchus labrax*. We studied their respective patterns of expression in order to determine which tissues are capable of melatonin biosynthesis and which are not. We also expressed recombinant Aanat1a and Aanat1b and determined their substrate preferences and kinetics. Finally, we focused attention on the retina and pineal gland, the two main sites of melatonin biosynthesis, in order to determine how the enzymes distribute at the cellular level.

## **MATERIAL AND METHODS**

## **Animals**

Adult sea bass (*D. labrax*, L.) were obtained from “Méditerranée Pisciculture” (Salses, France) or the “Laboratorio de Cultivos Marinos” (CASEM, University of Cádiz, Puerto Real, Spain). Animals were maintained under natural conditions of photoperiod and temperature for at least three weeks in seawater at the laboratory. Fish were killed by decapitation either during day or under dim red light at night. All experiments were performed according to the European Union regulations concerning the protection of experimental animals. Animal experimental protocols were approved by the Animal Care and Use Committee of the Observatoire Océanologique of Banyuls sur Mer (CNRS-UPMC; authorization # A-66-01-601) and University of Cadiz (authorization # 5-2014).

## **Tissue processing**

The tissues used for the cloning, polymerase chain reaction (PCR) and real time quantitative PCR (qPCR), were immediately frozen in liquid nitrogen after sampling and stored at -80°C. The tissues to be used for the *in situ* hybridization were sampled at midnight and fixed overnight in freshly prepared 4% paraformaldehyde (PFA) in phosphate buffer saline (PBS; pH 7.2, 10 mM Na<sub>2</sub>HPO<sub>4</sub>, 1.8 mM KH<sub>2</sub>PO<sub>4</sub>) at +4°C. After fixation, they were washed in PBS and then dehydrated in an ethanol series (70%: 2 x 10 min; 95%: 2 x 10 min; 100%: 3 x 10 min), dipped for 10 min in butanol and then embedded in Paraplast (Sigma-Aldrich; Saint Quentin Fallavier, France).

## **Cloning strategy and RT-PCR amplification from different tissues**

Total RNA was extracted using the Trizol® method (Invitrogen; Cergy Pontoise, France) and used as a template to synthesize first strand cDNAs with Primescript Reverse transcriptase (Takara; Otsu, Japan). Retinal extracts and degenerated primers (Eurofins Genomics; Les Ullis, France) ([Supplementary Table 1](#)) were used to clone *aanat1a*, *aanat1b*

as well as *asmt*. Other details are indicated in [Supplementary Material and Methods 1](#) and [supplementary tables 2 and 3](#).

### **Quantitative real time PCR amplification**

Tissues were collected at noon (12:00 GMT+2h) and midnight (24:00 h GMT+2h) and cDNA were obtained from RNA after extraction as described above, using the Primescript reverse transcriptase (Takara; Otsu, Japan). Real time gene expression analysis was performed using the Roche-Diagnostics Light Cycler 2.0 (Meylan, France). The primers used for the sequences of interest, including the reference gene (L17; GenBank accession number AF139590.1), are given in [Supplementary Table 4](#) and the PCR were performed using the lightcycler Fast start DNA master SYBRgreen I kit (Roche Diagnostics; Meylan, France) with the following conditions: 95°C (1 min) and 40 cycles of 95°C (30 sec), 56°C (1 min) and 72°C (45 sec).

All experiments were duplicated (n = 5 [first series of experiments] or n = 3 [second series of experiments]). Because the sea bass pineal glands are very small, pools of 15 glands were used in each sample.

### ***In situ* hybridization**

Eight  $\mu\text{m}$  paraffin sections were obtained from the pineal glands sampled at midnight; the sections were mounted on slides coated with 3-aminopropyltriethoxysilane (2%; Sigma; Saint Quentin Fallavier, France). *In situ* hybridization was performed, and digoxigenin-labeled sense or anti-sense riboprobes were generated, using a commercially available kit (Roche Diagnostics; Meylan, France) according to the manufacturer's instructions. The *aanat1a* probe generated corresponded to bp 1-589. The *aanat1b* probe corresponded to bp 541-1639. The *asmt* probe corresponded to bp 572-807. The sense and anti-sense *aanat2*, probes match with the complete ORF (618 pb). The primers used to

generate the probes are listed in [Supplementary Table 5](#). The hybridization process was as detailed elsewhere [2] using a probe concentration of 1 µg/ml.

### **Production and purification of recombinant enzymes**

The *aanat1a* and *aanat1b* sequences cloned from the sea bass retina were sub-cloned into a pGEX4T1 expression plasmid (Novagen, EMD Chemicals Inc; Philadelphia, PA) containing a GST (glutathione S-transferase) tag. The production protocol was as detailed in [Supplementary Material and Methods 2](#).

### **AANAT activity assays**

Activity of GST-Aanat1a and GST-Aanat1b proteins was measured using a validated colorimetric assay [9] as detailed in the [Supplementary Material 3](#).

### **Data analysis and graphs**

The data from the kinetics studies were analyzed using the Prism6.01 software (GraphPad Software<sup>TM</sup>; San Diego, CA). For each saturation curve the best fitted equation was calculated using the extra sum of square F test, implemented in Prism. These were used to estimate the  $K_M$  (substrate concentration for which half of maximal velocity [ $V_{max}$ ] is reached), turnover number ( $k_{cat} = V_{max} / [Enzyme]$ ) and catalytic efficiency ( $k_{cat}/K_M$ ). The 95% confidence intervals (CI) were calculated for both the  $K_M$  and  $k_{cat}$ . The 95% CI of the ratio  $k_{cat}/K_M$  was calculated using an online calculator implemented on the Graphpad website ([www.graphpad.com](http://www.graphpad.com)). The 95% CI is displayed in the graphs for each kinetics constant in order to simplify direct comparison, as values which exhibited no overlap of their CI were considered as significantly different [14].

All drawings were performed using Prism6.01. Analyses of the effects of temperature on the activity of the recombinant Aanat1a and Aanat1b were done using the Two-Way ANOVA followed by a multiple  $t$  test comparison of means. Analyses of the day/night

variations of *aanat* expression (qPCR) were done using InStat3 from GraphPad™ and the unpaired *t* test (two-tail). Results were represented as the mean ± standard deviation (S.D.) or ± standard error of the mean (S.E.M.) as indicated in the figure legends.

## RESULTS

### Characteristics of *aanat1a*, *aanat1b*, *aanat2* and *asmt*

*aanats*. The *aanat1a*, *aanat1b* and *aanat2* sequences cloned were 1248, 1641 and 618 nucleotides in length ([Supplementary Figs 1, 2](#)), and encode 202, 226 and 206 aa peptides, respectively ([Supplementary Figure 2](#); Acc. #: EU378922, EU378923.1, KP954654, respectively). The *aanat2* has been identified in the sea bass genome (DLA\_VIII\_005510|*aanat2*|arylalkylamine *N*-acetyltransferase |LG8|11349220|11350343; [15]). At the protein level, the identity of Aanat1a and Aanat1b was 87-96% with other teleost Aanat1, 78-85% between them, and 62-74% with teleost Aanat2 (including sea bass Aanat2; [Supplementary Fig. 2](#)) and mammalian Aanat.

The three sea bass Aanat protein sequences obtained here displayed the characteristic conserved catalytic domains of the vertebrates' Aanat family, the AcCoA binding domains A and B, and the substrate binding domains C and D [16]. In addition, all three sequences exhibited conserved residues known to be important for the enzyme activity and regulation; these include a lysine located close to the N-terminus, the protein kinase A phosphorylation sites on both ends of the molecules, a “CPL” peptide sequence in a floppy loop within the binding region, and closely positioned histidine and proline residues in the active site ([Supplementary Fig. 2](#)) (for details see [16-18]). A unique feature of Aanat1b was a 21 aa tail in the C terminal, absent from the Aanat1a and Aanat2 sequences. Another notable difference distinguishing Aanat2 from the other two enzymes was the presence of a

valine at position 112 and an isoleucine at position 158 instead of, respectively, a lysine and a methionine ([Supplementary Fig. 2](#)). These valine and isoleucine are involved in thermal stability and catalytic efficiency of teleost Aanat2 [10]. In a thorough analysis of the available teleost's Aanat sequences we found that these residues are highly conserved among teleost Aanat2 and, when not present, replaced by a valine. Conversely, while the corresponding lysine and methionine found in Aanat1a and Aanat1b are specific of this family and of Sarcopterygii Aanats.

*asmt*. The cloning strategy produced an 1146 nucleotides partial sequence covering the 3' untranslated end (KP986446). The coding sequence translates in a 269 aa peptide sequence ([Supplementary Fig. 3](#)). The nucleotide sequence produced significant alignments with only 3 Teleost fish sequences (using the Blastn at NCBI), namely the *asmt* from *S. maximus* and *T. nigroviridis* and the predicted *asmt* sequence from *O. niloticus*. (~70% coverage, ~85% identity within the corresponding covered regions). Compared to the other teleost Asmts, this partial *D. labrax* sequence lacks ~60 aa in the carboxyl end ([Supplementary Fig. 3](#)) but it was recognized as belonging to the superfamily of adenosyl methionine methyltransferases. Identity ranged between 50 and 60% within the corresponding fragments of the tetrapods' Asmt sequences. Analysis of the primary sequence indicates that Asmt from *D. labrax* possesses the conserved methyltransferase domain found in the vertebrates' Asmt family. The putative casein kinase II phosphorylation site was identified; the cysteine residues found at positions 37, 105, 118, 125 and 194 were also highly conserved ([Supplementary Fig. 3](#)).

#### **Kinetics of recombinant Aanat1a and Aanat1b**

The kinetics constants  $K_M$ ,  $k_{cat}$ , and  $k_{cat}/K_M$  from the recombinant Aanat1a and Aanat1b produced were calculated from the saturation curves performed with two

indoleethylamines (tryptamine and serotonin) and two phenyleethylamines (PEA and dopamine) (Fig. 1A). Both Aanat1a and Aanat1b displayed 2- to 3-fold lower  $K_M$  values (higher affinity) for indoleethylamines compared to phenyleethylamines (Fig. 1B).  $K_M$  for phenyleethylamines was around two times lower for Aanat1a than for Aanat1b. The  $k_{cat}$  fluctuated within the same range for all the enzymes and substrates except for the acetylation of phenyleethylamines by Aanat1b, which displayed lower values (Fig. 1B). Both Aanat1a and Aanat1b enzymes exhibited a better catalytic efficiency ( $k_{cat}/K_M$ ) with serotonin as a substrate (Fig. 1B). Aanat1a displayed equivalent  $k_{cat}/K_M$  for the three other substrates while Aanat1b exhibited lower catalytic efficiency for phenyleethylamines.

When looking at the responses of the recombinant enzymes to temperature, both Aanat1a and Aanat1b enzymes increased  $V_{max}$  with the increasing temperature from 0 to 37°C; above this threshold activity decreased abruptly (Fig. 2). These effects were highly significant. In addition, subtle differences were found between Aanat1a and Aanat1b activities at some temperatures only, particularly the extreme ones (Fig. 2).

#### **Tissue distribution of *aanat1a*, *aanat1b*, *aanat2* and *asmt***

The results of the RT-PCR performed in the different sea bass tissues are summarized in figure 3. Both Aanat1a and Aanat1b are expressed in the different brain areas and in the retina. Differences were observed among the peripheral tissues. Transcripts were identified in the gonad, intestine, liver and muscle (Aanat1a and Aanat1b), gills and heart (Aanat1b) (Fig. 3). Aanat1a and Aanat1b transcripts were also amplified from pineal extracts. Figure 4 shows in detail the products of the amplification of Aanat1a and Aanat1b transcripts using primers covering their respective ORF. The 609 and 681 bp long amplicons were sequenced to confirm their identity. In the same extracts, Aanat2 transcripts were detected almost exclusively in the pineal gland, traces being also found in the retina (Figs 3, 4). A significant

detection of *Asmt* transcripts was observed mainly in the retina and pineal organ (Figs 3, 4), while trace amounts were seen in the diencephalon and cerebellum (Fig. 3). No amplification signal was detected in the other tissues investigated.

### **Quantitative expression of *aanat1a* and *aanat1b* in retina and pineal complex**

Because both *aanat1a* and *aanat1b* transcripts are present in the pineal complex and retina, together with *Asmt*, we decided to investigate the cellular sites of expression in these different organs, with the aim to distinguish the cells that are capable of melatonin synthesis from those that are not. We first quantified the abundance of transcripts in these tissues in order to perform the *in situ* hybridization at the best time of the light/dark cycle. Independent of the tissue and enzyme considered, the levels of expression were higher at midnight than at midday (Fig. 5). Only *aanat1b* mRNA abundance displayed significant midday/midnight differences. Although comparison of relative amounts remains difficult, it seemed that both *aanat1a* and *aanat1b* transcript levels were higher in the retina compared to their respective counterparts in the pineal organ. While the relative levels of expression of *aanat1a* and *aanat1b* appeared similar in the pineal organ complex, this seemed not to be the case in the retina where *aanat1b* mRNA appeared ~100-fold more abundant than *aanat1a* (Fig. 5). Based on above results we decided to perform the *in situ* hybridization on organs sampled at midnight.

### **Localization of *aanat1a*, *aanat1b* and *asmt* in the retina**

In the retina we found that both *aanat1a* and *aanat1b* were expressed in the 3 nuclear layers, namely the outer nuclear (ONL), inner nuclear (INL) and ganglion cell (GCL) layers (Fig. 6). The differences were quantitative and in agreement with the qPCR data (see above). The *aanat1a* labeling covered the whole ONL from the basal lamina to the IPL; this corresponds to the position occupied by the cell bodies of the photoreceptors. No or very

weak labeling was observed in the inner segments located just above the outer limiting membrane, as seen in figure 6. Retinal cells of the INL were also labeled: some scattered cells were located at the most basal part of the INL where the amacrine cells are usually found; others occupied the position of the bipolar cells and Müller cell bodies, as they were located more in the center of the INL. Finally a few neurons of the GCL also expressed *aanat1a* (Fig. 6). The *Aanat1b* labeling was observed in the same areas. In contrast with *aanat1a*, *aanat1b* was strongly expressed in some inner segments of the photoreceptors, while other layers remained unstained (yellow arrows in Fig. 6). Also, in comparison with the *aanat1a* probe, the *aanat1b* probe provided a stronger and more extended labeling in the cells of the INL (basal and inner parts) and GCL. The labeling obtained with the *Asmt* probe was similar to that obtained with the *aanat1b* probe, except that inner segment of all the photoreceptor cells was labeled (Fig. 6).

#### **Localization of *aanat1a* and *aanat1b* in the pineal complex**

The finding that *aanat1a* and *aanat1b* transcripts were amplified from pineal extracts by RT-PCR was puzzling as it broke the dogma that the pineal gland enzyme is Aanat2. However, the sampling of the pineal gland includes in most cases the dorsal sac, as both tissues are closely attached one to each other [19]. We thus decided to investigate the sites of expression by *in situ* hybridization. It appeared that Aanat2 mRNA was indeed exclusively expressed in the pineal tissue (Fig. 7). While no or a very weak diffuse labeling was obtained with the *aanat1a* probe, a positive reaction was obtained with the *aanat1b* probe in some areas of the dorsal sac, surrounding the pineal organ, but not in the pineal gland itself (Fig. 7).

## **DISCUSSION**

This study in the European sea bass supports and extends *in silico* and experimental evidence that two Aanat1 enzymes are present in some fish, together with Aanat2 [8, 12, 13]. It provides totally new information concerning the tissue distribution, localization and kinetics of Aanat1a and Aanat1b. The two enzymes, together with Aanat2, possess the characteristics of the vertebrates' Aanat family of enzymes. The phylogenetic analysis clearly indicated that they are different isoforms (see also [8]). Aanat1b can be unambiguously distinguished not only from Aanat1a, but also from Aanat2, by the addition of 21 aa residues in the C terminal end. Altogether, our results agree with previous *in silico* analysis indicating that the Aanat1a/Aanat1b split resulted from the teleost-specific WDG [8].

The Aanat1a enzymes on the one hand, and Aanat1b enzymes on the other hand, displayed a high degree (95%) of conservation in the sea bass and sole, including the C terminal tail for the Aanat1b enzymes. The differences in the *S. senegalensis* and *D. labrax* 1a and 1b enzymes were seen at both ends of the protein; overall the enzymes displayed no more than 80% identity. These differences in the tails may have consequences at the level of the regulation of the enzyme stability and activity, particularly on the phosphorylation of TYR (RRHT end) and SER (RRNS end) residues that are of crucial importance in the process of the nocturnal activation of the enzyme (for details see [16]). Generally after a WGD one of the paralogs is lost unless it acquires new function or sub-functionalization. Regarding Aanat1, some teleost fish express either one of the forms or both of them. This suggests that in some species sub-functionalization occurred while in others it did not, eventually resulting in the loss of one of the paralogs in the latter case. The noticeable differences in the daily and developmental expression patterns of *aanat1a* and *aanat1b* in larvae, post-larvae, and adults of the sole suggest two enzymes have different functions in this species [13]. It was therefore of interest to investigate the kinetics and sites of expression of *aanat1a* and

aanat1b in sea bass to know more about their respective specific characteristics and function.

Aanat enzymes of vertebrates usually display a significantly higher catalytic efficiency for indoleethylamines vs. phenyleethylamines [5, 9, 10, 16]. We bring here evidence that Aanat1 enzymes acetylated both indole- and phenyl-ethylamines in accordance with our previous findings in other species [20-24]. In addition, Aanat1a and Aanat1b behaved similarly with regard to temperature; their optimum activity was reached at 37°C. This distinguishes all the vertebrates' Aanat from the teleost Aanat2 enzymes, as the latter exhibits different and species-dependent response patterns to temperature variation [6, 9, 11]. The subtle differences found between Aanat1a and Aanat1b enzymes responses, particularly at the low and high temperatures, might be related to the observed seasonal effects of temperature on the sea bass retinal and plasma melatonin rhythms [25]. Sea bass Aanat1a acetylated phenyleethylamines twice better than Aanat1b did (higher affinity and catalytic efficiency), whereas no difference was seen between the two forms with regard to indoleethylamines. Conversely, indoleethylamines had a slight inhibitory effect on Aanat1a activity at high concentrations, a characteristic shared with recombinant pike, sea bream and zebrafish Aanat1, the sequence of which indicates they belong to the 1a family [21, 24]. Altogether these data show that Aanat1a and Aanat1b can acetylate both serotonin and dopamine. The Aanat1a might be involved preferentially in the acetylation of dopamine while Aanat1b seems to prefer serotonin. The production of *N*-acetyldopamine (NAD) and *N*-acetylserotonin (NAS) will thus depend on the presence of the appropriate enzyme, the levels of expression of either enzyme, and the respective concentrations of the substrates in the areas where they are produced or released.

In order to better identify the respective roles of Aanat1a and Aanat1b we analyzed

their tissue distribution. We found that Aanat1 enzymes displayed a widespread distribution in central and peripheral tissues; differences were found in the distribution of the two isoforms and their relative expression levels. In contrast, the expression of Aanat2 and Asmt was much more restricted. We thus confirm in the sea bass that Aanat2 is a pineal enzyme mainly; the traces of amplicons detected in the retina were negligible compared to the intensity of the amplification seen in the pineal gland extracts. This was confirmed by quantitative PCR measurements (not shown). Similarly our data support the idea that Asmt is mainly a retinal and pineal enzyme in fish, although traces of expression were found in the diencephalon and cerebellum; no expression was detected in the peripheral tissues analysed. In the diencephalon, it cannot be excluded that the detection of Asmt mRNA was due to the presence of residual tissue elements from the pineal stalk; even after pineal gland removal, elements from the pineal stalk that connect the pineal end vesicle to the diencephalon may remain. It is also possible that melatonin is produced in local areas of the diencephalon and cerebellum, which also express melatonin receptors, consistent with the hypothesis that melatonin exerts autocrine/paracrine effects in these areas [26, 27]. Whatever it may be, the presence of either form of Aanat (1a/1b/2) together with Asmt in a given tissue, indicates it can synthesize melatonin, providing serotonin is present. If melatonin might be synthesized in the diencephalon and cerebellum, the main sites of production appear to be the retina and pineal gland; unless a second yet unidentified Asmt gene is expressed in the sea bass (as is the case in the goldfish [28]) no synthesis occurs in the peripheral tissues. It must then be assumed that in the other areas where they are expressed Aanat1a and 1b serve other functions than melatonin production, related to the metabolism of serotonin and dopamine. In brief, the enzymes may be part of the melatonin biosynthesis pathway or just involved in the catabolism of serotonin and/or dopamine. This

catabolism would help eliminating dopamine or serotonin not discarding the possibility that NAD and NAS, the end products, might have proper effects. These alternatives are discussed below putting emphasis on the pineal gland and retina.

The detection of all three forms of Aanat (1a/1b/2) in extracts from the sea bass pineal glands was puzzling because it is generally believed that Aanat2 is the main pineal enzyme (see above) and is part of the melatonin synthesis machinery in this tissue. The *in situ* hybridization unraveled the enigma because it appeared that Aanat1a and 1b were expressed in the dorsal sac, while Aanat2 was expressed in the pineal gland *stricto sensu*. The dorsal sac or *saccus dorsalis* of fish is a tissue closely associated to the pineal gland, particularly in the area of the pineal stalk, which connects to the brain. The dorsal sac and pineal gland are interconnected through the vasculature, and the lumen of each tissue is bathed by the cerebrospinal fluid (CSF) [19]. It has been suggested that the dorsal sac is an equivalent of the choroid plexus of mammals but very little is known on its function. In fish it works as a blood-CSF barrier [29]. Interestingly, the dorsal sac synthesizes neither serotonin nor dopamine [29]; and does not produce melatonin as no Asmt activity is present [30]. However, a monoamine oxidase (MAO) activity has been detected in the tissue [29, 31]. MAO is an enzyme involved in the catabolism of serotonin and dopamine. It is possible that Aanat1 enzymes of the dorsal sac help eliminating serotonin and dopamine from the CSF and blood, together with MAO. It is interesting that among other products the MAO pathway generates H<sub>2</sub>O<sub>2</sub>; this results in the production of reactive oxygen species toxic to the cell [32, 33]. Aanat1a and Aanat1b activities might thus be an alternative degradation pathway of monoamines that protects indirectly the tissues from the oxidative damage induced by the MAO activity. They might also have direct protective effects by virtue of the intrinsic antioxidant properties of the end products NAS and NAD [34, 35]. The presence of

Aanat1a and Anaat1b in the dorsal sac is thus beneficial in many respects. The blood and CSF are pathways for the dissemination of NAD and NAS to other parts of the brain and body. The above comments may apply to other tissues where serotonin and dopamine are produced or released such as the liver and intestine [36]. As the dorsal sac receives no innervation, the midday/midnight variations in *aanat1b* expression detected here must be due either to a direct photosensitivity of its epithelial cells or to regulation by some rhythmic signal from the blood or CSF. Assuming that Anaat1b mRNA variations reflect the variations in the amount of protein as is the case for Anaat2, the higher levels at night may reflect a higher catabolism of serotonin. In brief, the pineal gland of the sea bass expresses Anaat2; it is the site where melatonin is produced, while the surrounding *saccus dorsalis* expresses Anaat1 enzymes and has other functions.

In the retina, the metabolism of monoamines is very complex. The organ is another main site of active monoamines metabolism, melatonin being only one aspect of this metabolism. A previous study in the trout demonstrated that melatonin production occurs in the 3 nuclear layers, but is far stronger in the ONL compared to the INL and GCL [2]. It was therefore not surprising to find expression of Anaat1 (1a and 1b) and Asmt in the same cell types of the sea bass retina. For an extensive discussion on the synthesis of melatonin by the fish retina, the reader is referred to Besseau and co-workers [2]. In the trout however, only one Anaat1 enzyme was identified, while in the sea bass both Anaat1a and Anaat1b might be involved in the synthesis of melatonin. We found subtle differences between *Aaanat1a* and *Aaanat1b* expressions at two levels: the intensity and cellular distribution of the labeling. The *Aaanat1b* mRNA was more abundant than *Aaanat1a* mRNA, and displayed a larger distribution, as deduced from the *in situ* hybridization and qPCR data. In addition, both were not distributed evenly in the cells. This perhaps reflects functional differences between the

two isoforms of *Aanat1* that need to be explored.

From an evolutionary standpoint, the wide distribution of *Aanat* in the retina of Chondrichthyes and Teleost fish contrasts with the situation described in the retina of tetrapods where *Aanat* expression was found either in the INL (primates, cow and frog [37, 38]) or the GCL (chicken and rat [39, 40]) and at quite low levels compared to expression in the ONL. This restricted distribution compared to the aquatic vertebrates suggests some modification or loss of function during evolution. It has been suggested that *Aanat* serves other functions than melatonin production in the INL and GCL, because *Asmt* is absent [37]. The roles of *Aanat1* enzymes in the fish retina might not be restricted to the synthesis of melatonin and may more generally concern the metabolism of serotonin and dopamine. Both monoamines are neurotransmitters produced by distinct subsets of amacrine cells in the INL [41-44]. And, once released they may be taken up by other retinal cell types, including bipolar, ganglion and Muller cells [42, 45-48]. These and our data indicate that retinal monoamines and *Aanat* enzymes may co-localize in the retina but not only for melatonin production.

One characteristic of the retinal monoamine metabolism is its rhythmicity and the interplay between melatonin and dopamine along the 24 h light/dark cycle [49]. This melatonin/dopamine interplay regulates a number of rhythmic processes in the tissue. It is possible that *Aanat1a* and *Aanat1b* contribute to fine tuning dopamine and serotonin levels along the 24 h light/dark cycle. As discussed above for the dorsal sac, the enzymes may also help protecting the retina from oxidative damage. In addition to the effects of MAO activity discussed above, serotonin and dopamine can form toxic complexes with retinaldehyde [50, 51]; they can also bind covalently to polyunsaturated fatty acids (docosahexaenoic acid (DHA) and arachidonic acid (AA); [52-54]). DHA and AA are found in high amounts in the

retina and are essential for maintaining the structure and function of photoreceptors (refs in [16]). Accordingly, acetylation of serotonin and dopamine in the retina would prevent the formation of complexes with retinaldehyde, DHA or AA, and thus favor retinal structure and function [16, 50]. The large distribution of Aanat1a and Aanat1b is thus beneficial in many respects in the retina and probably also in other tissues where DHA and AA are important.

In addition to preventing from oxidative damage, it has been shown that NAS ensures neuroprotection through direct activation of the TrkB receptor in the retina and brain [55, 56]. In the retina the effects are circadian rhythms and associated to neurogenesis and cell proliferation. A remarkable feature of the fish retina is that it grows throughout the fish life and that the generation of new cells is a daily phenomenon [57]. Future studies will aim at investigating whether NAS plays a role in the daily generation of cells from the progenitors located in the ciliary margin zone and INL of the fish retina.

Finally, besides their important role in the clearance of indoleamines, neuroprotection and cell division, information accumulates suggesting the end products, NAS and NAD, may modulate enzyme activities including tryptophan hydroxylase [58] and dopamine hydroxylase [32], thus suggesting they might be part of a feedback loop within the monoamines metabolic pathways. NAD also stimulates methenyltetrahydrofolate synthase, which is important in the folate metabolism [59]). Interestingly, studies in the mammalian retina indicate that methyltetrahydrofolate can be excited by light and is one cofactor of cryptochromes, which are part of the molecular clock machinery [60]. Thus, aanat1 activity indirectly contributes to circadian photoreception in the eye.

In conclusion this study describes a new situation in teleost fish concerning the Aanat family of enzymes. For the first time since their existence was discovered [12] we characterized the Aanat1a and Aanat1b enzymes, described their distribution and quantified

their expression in the retina and pineal gland. Our data support and add to previous studies suggesting a wide and complex role for Aanat1 enzymes in the whole body organization. The enzymes catalyze the production NAD and NAS, which may just be catabolites of serotonin and dopamine not discarding the possibly that they might have proper effects, that need now to be investigated in fish.

**Acknowledgements:**

This study was supported by the French Research National Agency (ANR, Grant 07-BLAN-0097-01, TEMPANAT), the CNRS, IFREMER, UPMC-Paris6 (GDR2821, UMR7232) and Junta de Andalucía (P10-AGR-05916).

## REFERENCES

1. FALCÓN J, BESSEAU L, SAUZET S et al. Melatonin effects on the hypothalamo-pituitary axis in fish. *Trends Endocrinol Metab* 2007; **18**:81-88.
2. BESSEAU L, BENYASSI A, MØLLER M et al. Melatonin pathway: breaking the 'high-at-night' rule in trout retina. *Exp Eye Res* 2006; **82**:620-627.
3. KLEIN DC Arylalkylamine *N*-acetyltransferase: "the timezyme". *J Biol Chem* 2007; **282**:4233-4237.
4. FALCÓN J, GUERLOTTÉ JF, VOISIN P et al. Rhythmic melatonin biosynthesis in a photoreceptive pineal organ: a study in the pike. *Neuroendocrinology* 1987; **45**:479-486.
5. KLEIN DC, COON SL, ROSEBOOM PH et al. The melatonin rhythm-generating enzyme: molecular regulation of serotonin *N*-acetyltransferase in the pineal gland. *Recent Prog Hormone Res* 1997; **52**:307-357.
6. FALCÓN J Cellular circadian clocks in the pineal. *Prog Neurobiol* 1999; **58**:121-162.
7. FALCÓN J, BESSEAU L, BOEUF G. Molecular and cellular regulation of pineal organ responses. In: *Sensory systems neuroscience - Fish physiology*. Hara T, Zielinski B eds., AP Elsevier, 2007; pp. 243-306.
8. CAZAMÉA-CATALAN D, BESSEAU L, FALCÓN J et al. The Timing of Timezyme Diversification in Vertebrates. *PLoS Biol* 2014:1-22.
9. CAZAMÉA-CATALAN D, MAGNANOU E, HELLAND R et al. Functional diversity of Teleost arylalkylamine *N*-acetyltransferase-2: is the *timezyme* evolution driven by habitat temperature? *Molec Ecol* 2012; **21**:5027–5041.
10. CAZAMÉA-CATALAN D, MAGNANOU E, HELLAND R et al. Unique arylalkylamine *N*-acetyltransferase-2 polymorphism in salmonids and profound variations in thermal stability and catalytic efficiency conferred by two residues. *J Exp Biol* 2013; **216**:1938-1948.
11. FALCÓN J, MIGAUD H, MUÑOZ-CUETO JA et al. Current knowledge on the melatonin system in teleost fish. *Gen Comp Endocrinol* 2010; **165**:469-482.
12. COON SL, KLEIN DC Evolution of arylalkylamine *N*-acetyltransferase: Emergence and divergence. *Mol Cell Endocrinol* 2006; **252**:2-10.
13. ISORNA E, ALIAGA-GUERRERO M, EL M'RABET A et al. Identification of two arylalkylamine *N*-acetyltransferase 1 genes with different developmental expression profiles in the flatfish *Solea senegalensis*. *J Pineal Res* 2011; **51**:434-444.

14. CUMMING G, FIDLER F, VAUX DL Error bars in experimental biology. *J Cell Biol* 2007; **177**:7-11.
15. MCSTAY E, MIGAUD H, MARIA VERA L et al. Comparative study of pineal clock gene and AANAT2 expression in relation to melatonin synthesis in Atlantic salmon (*Salmo salar*) and European seabass (*Dicentrarchus labrax*). *Comp Biochem Physiol A-Molec & Integr Physiol* 2014; **169**:77-89.
16. FALCÓN J, COON SL, BESSEAU L et al. Drastic neofunctionalization associated with evolution of the “timezyme” AANAT 500 million years ago. *Proc Natl Acad Sci USA* 2014; **111**:314–319.
17. HICKMAN AB, KLEIN DC, DYDA F Melatonin biosynthesis: The structure of serotonin *N*-acetyltransferase at 2.5 Å resolution suggests a catalytic mechanism. *Molec Cell* 1999; **3**:23-32.
18. PAVLICEK J, COON SL, GANGULY S et al. Evidence that proline focuses movement of the floppy loop of arylalkylamine *N*-acetyltransferase (EC 2.3.1.87). *J Biol Chem* 2008; **283**:14552-14558.
19. FALCÓN J L'organe pinéal du Brochet (*Esox lucius*, L.) I. Etude anatomique et cytologique. *Reprod Nutr Dev* 1979; **19**:445-465.
20. BENYASSI A, SCHWARTZ C, COON SL et al. Melatonin synthesis: arylalkylamine *N*-acetyltransferases in trout retina and pineal organ are different. *Neuroreport* 2000; **11**:255-258.
21. COON SL, BÉGAY V, DEURLOO D et al. Two arylalkylamine *N*-acetyltransferase genes mediate melatonin synthesis in fish. *J Biol Chem* 1999; **274**:9076-9082.
22. ZILBERMAN-PELED B, BENHAR I, COON SL et al. Duality of serotonin-*N*-acetyltransferase in the gilthead seabream (*Sparus aurata*): molecular cloning and characterization of recombinant enzymes. *Gen Comp Endocrinol* 2004; **138**:139-147.
23. ZILBERMAN-PELED B, BRANSBURG-ZABARY S, KLEIN DC et al. Molecular evolution of multiple arylalkylamine *N*-acetyltransferase (AANAT) in fish. *Marine Drugs* 2011; **9**:906-921.
24. ZILBERMAN-PELED B, RON B, GROSS A et al. A possible new role for fish retinal serotonin-*N*-acetyltransferase-1 (AANAT1): Dopamine metabolism. *Brain Res* 2006; **1073-1074**:220-228.
25. GARCIA-ALLEGUE R, MADRID JA , SANCHEZ-VAZQUEZ FJ Melatonin rhythms in European sea bass plasma and eye: influence of seasonal photoperiod and water temperature. *J Pineal Res* 2001; **31**:68-75.

26. BAYARRI MJ, GARCIA-ALLEGUE R, MUÑOZ-CUETO JA et al. Melatonin binding sites in the brain of European sea bass (*Dicentrarchus labrax*). *Zool Sci* 2004; **21**:427-434.
27. HERRERA-PEREZ P, RENDON MD, BESSEAU L et al. Melatonin receptors in the brain of the European sea bass: An *in situ* hybridization and autoradiographic study. *J Comp Neurol* 2010; **518**:3495-3511.
28. VELARDE E, CERDA-REVERTER JM, ALONSO-GOMEZ AL et al. Melatonin-synthesizing enzymes in pineal, retina, liver, and gut of the goldfish (*Carassius auratus*): mRNA expression pattern and regulation of daily rhythms by lighting conditions. *Chronobiol Int* 2010; **27**:1178-1201.
29. JANSEN WF Structure and function of the paraphysis cerebri in the rainbow-trout, *Salmo gairdneri richardson* - a histological, cytochemical, enzyme-cytochemical, ultrastructural and autoradiographic study. *Cell Tissue Res* 1985; **242**:127-143.
30. FALCÓN J, BÉGAY V, GOUJON JM et al. Immunocytochemical localization of hydroxyindole-*O*-methyltransferase in pineal photoreceptor cells of several fish species. *J Comp Neurol* 1994; **341**:559-566.
31. FALCÓN J, JUILLARD MT , COLLIN JP L'organe pinéal du Brochet (*Esox lucius*, L.). IV. Sérotonine endogène et activité monoamine oxydasique; étude histochimique, ultracytochimique et pharmacologique. *Reprod Nutr Develop* 1980; **20**:139-154.
32. KUHN DM, ARTHUR R Dopamine inactivates tryptophan hydroxylase and forms a redox-cycling quinoprotein: Possible endogenous toxin to serotonin neurons. *J Neurosci* 1998; **18**:7111-7117.
33. SIRAKI AG , O'BRIEN PJ Prooxidant activity of free radicals derived from phenol-containing neurotransmitters. *Toxicology* 2002; **177**:81-90.
34. OXENKRUG GF, REQUINTINA PJ *N*-acetyldopamine inhibits rat brain lipid peroxidation induced by lipopolysaccharide. *Ann NY Acad Sci* 2005; **1053**:394-399.
35. PERIANAYAGAM MC, OXENKRUG GF, JABER BL Immune-modulating effects of melatonin, *N*-acetylserotonin, and *N*-acetyldopamine. *Ann NY Acad Sci* 2005; **1053**:386-393.
36. NISEMBAUM LG, TINOCO AB, MOURE AL et al. The arylalkylamine-*N*-acetyltransferase (AANAT) acetylates dopamine in the digestive tract of goldfish: A role in intestinal motility. *Neurochem Int* 2013; **62**:873-880.

37. COON SL, DEL OLMO E, YOUNG WS, 3RD et al. Melatonin synthesis enzymes in *Macaca mulatta*: focus on arylalkylamine *N*-acetyltransferase (EC 2.3.1.87). *J Clin Endocrinol Metab* 2002; **87**:4699-706.
38. ISORNA E, BESSEAU L, BOEUF G et al. Retinal, pineal and diencephalic expression of frog arylalkylamine *N*-acetyltransferase-1. *Molec Cell Endocrinol* 2006; **252**:11-18.
39. GARBARINO-PICO E, CARPENTIERI AR, CONTIN MA et al. Retinal ganglion cells are autonomous circadian oscillators synthesizing *N*-acetylserotonin during the day. *J Biol Chem* 2004; **279**:51172-51181.
40. LIU C, FUKUHARA C, WESSEL JH et al. Localization of AANAT mRNA in the rat retina by fluorescence *in situ* hybridization and laser capture microdissection. *Cell Tissue Res* 2004; **315**:197-201.
41. DUNKER N Development and organization of the retinal dopaminergic system of *Ichthyophis kohtaoensis* (Amphibia; Gymnophiona). *Cell Tissue Res* 1997; **289**:265-274.
42. GHAI K, ZELINKA C, FISCHER AJ Serotonin released from amacrine neurons is scavenged and degraded in bipolar neurons in the retina. *J Neurochem* 2009; **111**:1-14.
43. MENG S, RYU S, ZHAO B et al. Targeting retinal dopaminergic neurons in tyrosine hydroxylase-driven green fluorescent protein transgenic zebrafish. *Molec Vision* 2008; **14**:2475-2483.
44. POZDEYEV N, TOSINI G, LI L et al. Dopamine modulates diurnal and circadian rhythms of protein phosphorylation in photoreceptor cells of mouse retina. *Europ J Neurosci* 2008; **27**:2691-2700.
45. CHENG Z, ZHONG YM, YANG XL Expression of the dopamine transporter in rat and bullfrog retinas. *Neuroreport* 2006; **17**:773-777.
46. KUBRUSLY RCC, PANIZZUTTI R, GARDINO PF et al. Expression of functional dopaminergic phenotype in purified cultured Muller cells from vertebrate retina. *Neurochem Int* 2008; **53**:63-70.
47. POW DV, COOK DK Tryptophan is present in glial cells and photoreceptors in the chicken retina. *Neuroreport* 1997; **8**:1767-1770.
48. REIS RAD, VENTURA ALM, SCHITINE CS et al. Muller glia as an active compartment modulating nervous activity in the vertebrate retina: Neurotransmitters and trophic factors. *Neurochem Res* 2008; **33**:1466-1474.

49. MCMAHON DG, IUUVONE PM , TOSINI G Circadian organization of the mammalian retina: From gene regulation to physiology and diseases. *Prog Ret Eye Res* 2014; **39**:58-76.
50. KLEIN DC Evolution of the vertebrate pineal gland: The AANAT hypothesis. *Chronobiol Int* 2006; **23**:5-20.
51. PEZZELLA A, PROTA G Formation of novel tetrahydroisoquinoline retinoids by Pictet-Spengler reaction of dopamine and retinaldehyde under conditions of relevance to biological environments. *Tetrahedron Let* 2002; **43**:6719-6721.
52. PETERS GH, WANG C, CRUYS-BAGGER N et al. Binding of serotonin to lipid membranes. *J Am Chem Soc* 2013; **135**:2164-2171.
53. LIU X, YAMADA N, MARUYAMA W et al. Formation of dopamine adducts derived from brain polyunsaturated fatty acids mechanism for Parkinson disease. *J Biol Chem* 2008; **283**:34887-34895.
54. VERHOECKX KCM, VOORTMAN T, BALVERS MGJ et al. Presence and formation of putative biological activities of *N*-acylserotonins, a novel class of fatty-acid derived mediators, in intestinal tract. *BBA Lip Lip Metab* 2011; **1811**:578-586.
55. IUUVONE PM, BOATRIGT JH, TOSINI G et al. *N*-acetylserotonin: circadian activation of the BDNF receptor and neuroprotection in the retina and brain. *Adv Exp Med Biol* 2014; **801**:765-771.
56. TOSINI G, YE K, IUUVONE PM *N*-acetylserotonin: Neuroprotection, neurogenesis, and the sleepy brain. *Neuroscientist* 2012; **18**:645-653.
57. CHIU JF, MACK AF, FERNALD RD Daily rhythm of cell-proliferation in the teleost retina. *Brain Res* 1995; **673**:119-125.
58. KUHN DM, ARTHUR RE, THOMAS DM et al. Tyrosine hydroxylase is inactivated by catechol-quinones and converted to a redox-cycling quinoprotein: Possible relevance to Parkinson's disease. *J Neurochem* 1999; **73**:1309-1317.
59. ANGUERA MC, STOVER PJ Methenyltetrahydrofolate synthetase is a high-affinity catecholamine-binding protein. *Arch Biochem Biophys* 2006; **455**:175-187.
60. WOLF G Three vitamins are involved in regulation of the circadian rhythm. *Nutr Reviews* 2002; **60**:257-260.

## FIGURE LEGENDS

**Figure 1.** Kinetics of *D. labrax* AANAT1a and AANAT1b recombinant enzymes. **A:** Saturation curves were obtained with increasing concentrations of substrate as indicated in the abscissae (one representative experiment out of 3 to 5); mean  $\pm$  S.E.M. (n = 3). **B:** Kinetics constants -  $k_M$ ,  $k_{cat}$ , and  $k_{cat}/k_M$  - were measured at 35°C for tryptamine, serotonin, dopamine, and PEA; mean  $\pm$  95% confidence interval (n = 24). For details see materials and methods.

**Figure 2.** Effects of temperature on Vmax of AANAT1a and AANAT1b from *D. labrax* recombinant enzymes. The activities of the recombinant enzymes were measured at the temperatures indicated, all other conditions being identical. Mean  $\pm$  S.D. (n = 3) from one out of two representative experiments. Two-Way ANOVA indicated significant effects of temperature ( $P < 0.0001$ ) that varied depending on the enzyme (interaction significant at  $P < 0.0001$ ). The mean by mean comparison was performed for each temperature and differences significant at  $P < 0.05$  or below are marked by \*.

**Figure 3.** Tissue specific expression of *D. labrax aanat1a*, *aanat1b* and *asmt* transcripts in different tissues. Specific primers were used to amplify cDNA from different tissue extracts (see materials and methods). From left to right: M: Molecular weight markers; C: controls (cDNA replaced by water); Cer: cerebellum; Di: diencephalon; OT: optic tectum; Tel: telencephalon; P: pineal complex; Pit: pituitary gland; R: retina; B: blood cells; Gj: gill; Go: gonad; H: heart; I: intestine; K: kidney; L: liver; Mu: muscle; S: skin. All the PCR bands were extracted, cDNA were sub-cloned and sequenced to verify their identity.

**Figure 4.** Expression of *D. labrax Aanat1a*, *Aanat1b*, *Aanat2* and *Asmt* transcripts in the pineal complex (P) and retina (R). Specific primers were used to amplify cDNA from pineal

gland and retina tissue extracts (see materials and methods). All products were sub-cloned and sequenced to verify their identity. M: Molecular weight standards. In the controls (C) cDNA was replaced by water.

**Figure 5.** Quantitative real time PCR amplification of *aanat1a* and *aanat1b* in the retina and pineal complex (pineal gland + dorsal sac). Each value represents the mean  $\pm$  S.E.M. of  $n = 5$  individuals. In the pineal complex each pineal value was obtained from a pool of 15 glands. Ribosomal L17 gene was used as housekeeping gene. Differences among groups were analyzed by the unpaired paired *t* test. Noon: white bars; midnight: black bars.

**Figure 6.** Expression of *D. labrax aanat1a*, *aanat1b*, and *asmt* transcripts in the retina by *in situ* hybridization. Sections were hybridized with an antisense probe directed against one of the enzymes mentioned on the top; controls were obtained with a sense probe for each of the mRNA tested. *Aanat1a* antisense probes: expression is seen in the photoreceptor cell bodies (double arrow) of the outer nuclear layer (ONL). Note the intense labeling at both ends of the ONL corresponding, respectively, to the outer limiting membrane and outer plexiform layer (OPL). In the inner nuclear layer (INL), cells occupying the position of the bipolar (horizontal arrow) and amacrine (upwards vertical arrow) cells are also labeled. A few cells are also labeled in the ganglion cell layer (GCL; downwards vertical arrow). *Aanat1b* antisense probe: expression is seen in the same layers than those described above for *aanat1a* (arrows) although it seems more extended. Note that the cell bodies of photoreceptors are more weakly labeled; in contrast, a strong labeling is detected in some, but not all, inner segments of photoreceptors (white downwards arrows). *asmt* antisense probe: same as for *aanat1b*; note that inner segment of all photoreceptors are labeled. Control: Sense *aanat1b* probe; no labeling is seen. Similar results were obtained with

*aanat1a* or *asmt* sense probes (not shown). IPL: inner plexiform layer; RPE: retinal pigment epithelium.

**Figure 7.** Localization of *D. labrax aanat1a*, *aanat1b* and *aanat2* transcripts in the pineal gland (P) and dorsal sac (ds) by *in situ* hybridization. Sections from glands sampled at midnight were hybridized with an antisense probe directed against *aanat2*, *aanat1a* or *aanat1b* transcripts. Controls were obtained with a sense probe for each of the mRNA tested. A labeling was observed in the pineal cells (arrows) with the antisense *aanat2* probe. No pineal cell was labeled with either *aanat1a* or *aanat1b* antisense probes. With the latter, a staining is observed in cells of the dorsal sac (arrow heads).

## SUPPLEMENTARY MATERIAL AND METHODS

### ***Supplementary Material and Methods 1***

**Cloning.** The PCR was performed in a total volume of 25  $\mu$ l, using the Advantage 2 polymerase kit (Invitrogen; Mountain View, CA, USA), as follows: 95°C (1 min) followed by 10 cycles of denaturation at 94°C (20 sec), annealing at 42°C (1 min) and extension at 68°C (30 sec), and by another 30 cycles of denaturation at 94°C (10 sec), annealing at 37°C (1 min) and extension at 68°C (30 sec). The PCR products were resolved in a 1% agarose gel, purified using a gel extraction kit (NucleoSpin<sup>®</sup>, Machery-Nagel<sup>GmbH</sup>; Hoerd, France), and sub-cloned into pGEM-T Easy (Promega; Charbonnières, France). Several positive clones were obtained from DH5 $\alpha$  competent bacteria transformed by electroporation; sequencing was conducted by Cogenics (Meylan, France). This strategy allowed obtaining sequences of 270 bp long for *aanat1a* and *aanat1b*, and 235 bp long for *asmt*, which were identified by their high homology with the corresponding sequences of known *aanat* and *asmt* from other species. Specific primer sets were then designed for further extension by 5'-and 3'-rapid amplification of cDNA ends (RACE; SMART RACE cDNA amplification kit; Clontech; Palo Alto, CA, US) ([Supplementary Table 2](#)). The products obtained after the 5',3'-RACE were, respectively, 559 and 651 bp long for *aanat1a*, 416 and 1201 bp long for *aanat1b* and 645 and 565 bp long for *asmt*. They were submitted to a second round of PCR using nested primers ([Supplementary Table 2](#)). The full length Aanat2 sequence was obtained from pineal extracts using specific primers designed from previously published sea bass genomic data [15] ([Supplementary Table 3](#)). All sequences were aligned using ClustalW2 (<http://www.ebi.ac.uk/Tools/msa/clustalw2/>).

**RT-PCR amplification from different tissues.** Total RNA from the different tissues tested was extracted as described above, and 1  $\mu$ g RNA was incubated with 1 unit of DNase I (Roche

Diagnostics; Meylan, France) for 20 min at 37°C. DNase inactivation (10 min at 65°C) was followed by reverse transcription using Primescript Reverse transcriptase (Clontech; Mountain View, CA, USA) according to the supplier's protocol. The obtained cDNAs were submitted to PCR amplification using specific primers ([Supplementary Table 3](#)) as follows: 95°C (1 min), 10 cycles of 94°C (20 sec), 62°C (*asmt*)/63°C (*aanat1b*)/ 64.5°C (*aanat1a*) (1 min), 68°C (1 min), followed by 10 cycles of 94°C (10 sec), 60°C (*asmt*, *aanat1b*)/64.5°C (*aanat1a*) (1min), 68°C (1 min), and terminated with 7 min at 68°C. For *Aanat2* the conditions were 94°C (3 min), 30 cycles of 94°C (30 sec), 63°C (30 sec) and 72°C (1 min), and terminated by 1 cycle at 72°C (5 min). Nested PCR were performed for *aanat1a* and *1b* enzymes, using another set of specific primers ([Supplementary Table 3](#)) and the following conditions: 95°C (1 min), 10 cycles of 94°C (20 sec), 65°C (*Aanat1b*)/66°C (*Aanat1a*), 68° C (1 min), 10 cycles of 94°C (10 sec), 63°C (*aanat1b*)/64°C (*aanat1a*), 68°C (1 min) and terminated with 7 min at 68°C. In the controls, the template cDNA was replaced either by water or RNA. The PCR products were resolved in an agarose gel, in the presence of DNA size markers (DNA/Hinf I marker or 1kb DNA ladder; Promega; Charbonnières, France), and the fragments of the expected size were extracted, subcloned in pGEM-T Easy and sequenced as indicated above to confirm their identity.

### ***Supplementary Material and Methods 2***

**Production and purification of recombinant enzymes.** Plasmids were transformed in *Escherichia coli* BL21 Rosetta bacteria (Merck KGaA; Darmstadt, Germany). Bacteria were grown in 2 x 500 ml Luria-Broth medium at 37°C. Protein production was induced with 0.5 mM IPTG (isopropyl  $\beta$ -D-1-thiogalactopyranoside) overnight at 20°C. Subsequent steps were carried out at 4°C. Bacterial cultures were centrifuged for 10 min at 1,800 g. The bacterial pellet was then washed with 1X TBS (Tris Buffered Saline, 50 mM Tris and 150 mM NaCl, pH

8) and centrifuged for 10 min at 5,000 g. Pellets were suspended in 50 ml lyses buffer (TBS 1X + cOmplete® protease inhibitor cocktail tablets; Roche Diagnostics; Meylan, France) and sonicated on ice for 30 sec by alternating 10 sec on and off pulse episodes. The lysate was centrifuge for 30 min at 25,000 g after addition of 0.1% Tween and 1% Triton X100.

Purification was achieved using affinity to Glutathione Sepharose 4B beads (GE Healthcare Life Sciences; Velizy Villacoublay, France). All following steps were conducted at 4°C and beads were pelleted by a 2 min centrifugation at 500 g in between each step. The beads were then washed with 10 mL phosphate buffer saline (PBS) and saturated with 10 mL TBSTT (TBS pH 8, 0.1% Tween 20, 1% Triton X100) and 1% powdered milk. Beads were washed 2 times in 10 ml TBSTT before incubation for 1h with the supernatant recovered at the end of production step. Beads were then pelleted and the supernatant removed. After three TBSTT washes and one TBS wash respectively, the GST-Aanat1 fusion proteins were recovered by 10 min incubation in 1 ml elution buffer (Tris 50 mM, glutathione 10 mM); this step was repeated 6 times. Protein amount was measured using the Bradford colorimetric assay using Bovin Serum Albumin (BSA) as a standard.

### ***Supplementary Materials and Methods 3***

**Aanat activity assays.** Reactions were typically performed using 0.025 µg of GST-dlAanat1a, or 0.05 µg of dlAanat1b, in a 100 µl final volume of a phosphate buffer (0.2 M, pH 6.1) solution containing 0.025 g/l BSA, 1 mM acetyl-Coenzyme-A (AcCoA) and substrate concentrations ranging from 0.05 to 10 mM. Incubation was 10 min at 35°C for both enzymes. The reaction was then stopped with a solution made of 0.2 M phosphate buffer pH 6.1, containing 1 mM 5,5'-dithio-bis(2nitrobenzoic acid) (DTNB), 10 mM EDTA, and 3 M guanidine hydrochloride. After 5 min of incubation at room temperature the optical density of the colored reaction product was measured at 405 nm using an absorbance microplate

reader (ELx808, BioTek Instruments Inc, Colmar, France). The substrates used were tryptamine, serotonin, dopamine and phenylethylamine.

## Supplementary Tables

**Supplementary Table 1. List of degenerated primers used for cloning of *aanat1a*, *aanat1b* and *asmt***

<b><i>aanat</i></b>	
degAanat1-F	gtttgaratcgagagagargc
degAanat1-R	gatggagccyttgcctgctg
<b><i>Asmt</i></b>	
degAsmt-F	gattrrcttccakgaaggrg
degAsmt-R	gtctgcacmarcatgttcag

**Supplementary Table 2. List of primers used for the 3',5'RACE**

<b><i>aanat1a</i></b>	
5'RACE	catcaggatggagcctttgtcctgctggcg
5'RACE nested	atgtggactgtgggcccgtgaggcttatgg
3'RACE	tggtttgaggaggacgtctggtggctttc
3'RACE nested	accggaccttccgccagcaggacaaaggct
<b><i>aanat1b</i></b>	
5'NAT1b-RACE-F	tgtcctgggtcccagagagagccgatgataa
5'RACE nested	aaccagcccatggacagctctggacacag
3'NAT1b-RACE-F	ctgtgtccagagctgtccatgggctgggt
3'RACE nested	ttatcatcggctctctctgggaccaggaca
<b><i>aanat2</i></b>	
Forward	atgcaggtcagtggctcaccgttcct
Reverse	gcagccactgttccgccgtgcgtat
<b><i>asmt</i></b>	
5'Asmt-RACE-F	agctgtcctctctctgccctccgtctgta
5'RACE nested	actgggccagagccatcctcatacagca
3'Asmt-RACE-R	actggactgacgaacgcagcataga
3'RACE nested	caaaccaggaggtgctgtgct

**Supplementary Table 3. List of primers used for the amplification from tissue extracts**

<b><i>aanat1a</i></b>	
Forward	cagagtacgcggggacacta
Forward nested	gctcagtccttacgcgcagt
Forward ORF	atgtcggtggtgagcgcagt
Reverse	ttatgtggactgtgggcccg
Reverse nested	atggagagtcagggcatccg
Reverse ORF	tcaacagccactgttacggcgc
<b><i>aanat1b</i></b>	
Forward	gagcgaggagaggacagaag
Forward nested	gcaaagtcgtatgatgtccg
Forward ORF	atgtccgctcgttggcgc
Reverse	gtccaacagaaacagtaagcagc
Reverse nested	aacctgtgcagacatctcatct
Reverse ORF	tcatacatcaaggtgttcaccagt
<b><i>aanat2</i></b>	
Forward	atgcaggtcagtggctcaccgttcct
Reverse	gcagccactgttccgccgtgcgtat
<b><i>asmt</i></b>	
Forward	actggactgacgaacgcagcataga
Reverse	tcatgtctctttgagccccagcactgcatcg
<b><i>β-actin</i></b>	
Forward	ctggagaagagctaygagctc
Reverse	gtacatgggtggtaccdccaga

**Supplementary Table 4. List of primers used for real time quantitative PCR**

<b><i>aanat1a</i></b>	
Forward	agaggcttagcgcggat
Reverse	atgtggactgtgggcccgtga
<b><i>aanat1b</i></b>	
Forward	caacctcaccttcacagagatg
Reverse	gattgcttcactggtgcgc
<b><i>L17</i></b>	
Forward	tgatacggcagcggaagtc
Reverse	gactcctgcgttgtcttcaaa

**Supplementary Table 5. List of primers used for producing ISH probes**

<b><i>aanat1a</i></b>	
Forward	aagcagtggatatcaacgcagagt
Reverse	atgtggactgtgggcccgt
<b><i>aanat1b</i></b>	
Forward	atgtccgtcgttggcgc
Reverse	tcatacatcaaggtggtcaccagt
<b><i>aanat2</i></b>	
Forward	atgcaggtcagtggctcaccgttctt
Reverse	gcagccactgttccgccgtgcgtat
<b><i>asmt</i></b>	
Forward	actggactgacgaacgcagcataga
Reverse	tcatgtctctttgagccccagcactgcatcg

### **Supplementary Figures**

#### **Supplementary Figure 1. Nucleotide alignment of *D. labrax* *Aanat1a* and *Aanat1b* coding sequences.**

The stars indicate nucleotide identity. CLUSTAL 2.1 sequence alignment.

#### **Supplementary Figure 2. Amino acid sequence alignment of *D. labrax* *Aanat1a*, *Aanat1b* and *Aanat2*.**

Sea bass *Aanat1a* (EU378922), *Aanat1b* (EU378923) and *Aanat2* (KP954654) were aligned using ClustalW2.0. The three sequences show the typical organization of the vertebrates' *Aanat* family of enzymes: (1) the conserved AcCoA binding domains A and B are common to the superfamily of GCN5 acetyltransferases; (2) the substrate binding domains C and D are common to vertebrates' *Aanats*. Conserved amino acid residues known to be important for the enzymes function are colored and in bold: in bold red are the Protein Kinase A (PKA) phosphorylation sites; in bold pink are residues highly conserved among all *Aanat* enzymes, while the blue are specific of either *Aanat1* or *Aanat2* enzymes.

#### **Supplementary Figure 3. Alignment of *D. labrax* with selected vertebrates' *Asmt* peptide sequences**

Sequence identity between fish *Asmt* is marked by the pink squares. In bold are the eight highly conserved cystein residues important for disulphide bond formation, as well as the putative casein kinase II phosphorylation site. The methyltransferase domain covers residues 33 to 234 of the sea bass sequence (KP986446). *Anolis carolinensis* (predicted): XP003218855; *Danio rerio*: NP001108381; *Gallus gallus*: NP990674; *Macaca mulatta*: NP001028112; *Oreochromis niloticus* (predicted): XP003445350; *Scophthalmus maximus*: ABM21528.

**Supplementary Figure 1.**

```

dlAanat1a    ---ATGTCCGGTGGTGTGAGCGCAGTGCCGTTTCATGAAGCCGCTCCA--CATGCGCTCCCCGG 55
dlAanat1b    ATGATGTCCGTCGTTGGCGCGCAGCCTTTCATCAAACCAATGCAGCCAT-CAC-CTTCTG 58
              ***** ** ** ***** ** * ** * ** * ** * ** * ** *
dlAanat1a    TGCCGCAGGGCCGCC-----GCCACACGCTGCCGGCCAGCGAGTTCGCTCTCTCAGCC 109
dlAanat1b    TTTTCGCTGGCATACAAAGGAGACACACACTGCCTGCGAGCGAATTCCGACCGCTCAACA 118
              *   ***   ***   *           *   *****   *****   *   *****   *****   *   *****   *
dlAanat1a    CGGAGGACGCCATCAGTGTGTTTCGAGATCGAGAGAGAAGCCTTCATCTCAGTGTCCGGTG 169
dlAanat1b    CGCAAGATGCCATAAGCGTCTTTGAAATCGAGCGAGAAGCTTTTATTTTCAGTGTCCAGGTG 178
              ** * ** ***** ** ** ** * ** ***** ***** ** ** ***** *****
dlAanat1a    AGTGTCTCTCCACCTGGACGAGGTGCGTCACTTCTCACACTTTGTCCTGAGCTGTCTC 229
dlAanat1b    AGTGTCCCCTCCACCTGGATGAGGTGCGTCATTTCTCACACTGTGTCCAGAGCTGTCCA 238
              ***** ***** ***** ***** ***** ***** *****
dlAanat1a    TTGGCTGGTTTTGAGGAGGGACGCTCTGGTGGCTTTCATCATCGGCTCATTTGTGGGACCAGG 289
dlAanat1b    TGGGCTGGTTTTGAGGAGGGCCGGCTGGTGGCTTTTATCATCGGCTCTCTCTGGGACCAGG 298
              *   ***** ***** ***** ***** ***** ***** *   ***** *****
dlAanat1a    AGAGGCTTAGCGCGGATGCCCTGACTCTCCATAAGCCTCACGGGGCCACAGTCCACATCC 349
dlAanat1b    ACAGACTCACTACAGACGCACTGACTCTGCACAAGCCCTGCGGCTCAACCGTCCACATCC 358
              * ** * *   * ** ** ***** ** *****   *** * ** ***** *****
dlAanat1a    ACGTCTGGCTGTCCACCGGACCTTCCGCCAGCAGGACAAAGGCTCCATCCTGATGTGGC 409
dlAanat1b    ACGTCTCGCTGTCCATCGCACCTTCCAGGACAGGGCAAAGGTCCTCCTGATGTGGC 418
              ***** ***** ** ***** * ***** ***** ***** ***** *****
dlAanat1a    GCTACCTGCAGTACCTCCGCTGCCTGCCCTATGTCCGCCGTGCTGTGCTCATGTGTGAAG 469
dlAanat1b    GTTACCTGCAGTATCTCCGCTGCCTTCCCAACGTGCGCCGAGCAGTGTGCTGATGTGCGAAG 478
              *   ***** ***** ***** * ** ***** ** ***** ***** *****
dlAanat1a    ACTTCTGGTTCCCTTCTATCAGAAGTCTGGTTTTCAAGGTGC-AGGGCCCTAGTGACATC 528
dlAanat1b    ACTTCTCATTCCTTTTTACCGCAAGTCAGGCTTCAAGGTACTAGGGCGCT-GTGCCATC 537
              *****   *** ** ** *   ***** ** ***** *   ***** ** ** *****
dlAanat1a    ACGGTGGGGCCCCTCACCTTCATCGAGATGGTCTACCCAGTCAGGGGCCACGCCTTCATG 588
dlAanat1b    ACCGTGGCCAACCTCACCTTCACAGAGATGTGGTACCCCATCAGCGGCCACGCGTACATG 597
              ** ***** ***** ***** ***** ***** ***** ***** * *****
dlAanat1a    CGCCGTAACAGTG-----GCTGTTGA----- 609
dlAanat1b    CGGCGCAACAGTGAAGCAATCCGTTTCCCTCAGCATCCCTTGACTCTGCCACTGACAAAG 657
              ** ** ***** ** **
dlAanat1a    -----
dlAanat1b    ACTGGTGAACACCTTGATGTTGA 681

```

**Supplementary Figure 2.**

dlAanat2	-MQVSGS-PFLKPF <sup>FL</sup> LKTPVRV <sup>VN</sup> PLRQ <sup>RRHT</sup> LPASEFRNLTPQDAISVFEIEREA <sup>F</sup> VSV 58
dlAanat1a	-MSVVS <sup>AV</sup> PFMK <sup>PL</sup> HMRSP---VPQG-- <sup>RRHT</sup> LPASEFRSLSPEDAISVFEIEREA <sup>F</sup> ISV 54
dlAanat1b	MMSV <sup>VGA</sup> QPF <sup>IK</sup> PMQ <sup>P</sup> SPS---VSPGIQ <sup>RRHT</sup> LPASEFRPLNTQDAISVFEIEREA <sup>F</sup> ISV 57
	*.* .: **:**: .. * ***** *..:*****:*
	<b>Motif C</b>
dlAanat2	SGE <sup>CPL</sup> TLDEVLN <sup>FL</sup> GQCP <sup>EL</sup> SLGW <sup>FEE</sup> GQLVAFIIGSGWDKERLSQEAMTQH <sup>V</sup> PDTPT <sup>V</sup> 118
dlAanat1a	SGE <sup>CPL</sup> HLDEVRH <sup>FL</sup> TLCPE <sup>LS</sup> LGWFEE <sup>GRL</sup> VAFIIGSLWDQERLSADAL <sup>TL</sup> HKPHGPT <sup>V</sup> 114
dlAanat1b	SGE <sup>CPL</sup> HLDEVRH <sup>FL</sup> TLCPE <sup>LS</sup> MGWFEE <sup>GRL</sup> VAFIIGSLWDQDRLTTDAL <sup>TL</sup> HKPCGST <sup>V</sup> 117
	***** ***:** *****:*****:***** **::**:*:* * * * .**
	<b>Motif D</b>
dlAanat2	<sup>HI</sup> HVLSVHRHCR <sup>QQ</sup> GKGSILLWRYLQYLRCMPGLRRALLI <sup>C</sup> EDFLV <sup>PF</sup> Y <sup>L</sup> KAGFKKKGPS 178
dlAanat1a	<sup>HI</sup> HVLAVHRTFR <sup>QQ</sup> DKGSILMWRYLQYL <sup>R</sup> CLPYVRR <sup>AV</sup> LMCEDFLV <sup>PF</sup> Y <sup>Q</sup> KSGFKVQGPS 174
dlAanat1b	<sup>HI</sup> HVLAVHRTFR <sup>QQ</sup> GKGPILMWRYLQYL <sup>R</sup> CLPNVRR <sup>AV</sup> LMCEDFLI <sup>PF</sup> Y <sup>R</sup> KSGFKVLGRC 177
	*****:*** ***.**.*:*****:* :***.*:*****.*** *:*** *
	<b>Motif A</b> <span style="float: right;"><b>Motif B</b></span>
dlAanat2	AISVSNMNFQEMEYMLGGQAYAR <sup>RNS</sup> GC----- 206
dlAanat1a	DITVGPLTFIEMVYPVRGHAFM <sup>RNS</sup> GC----- 202
dlAanat1b	AITVANLTFTEMWYPI <sup>S</sup> GHAYM <sup>RNS</sup> EAIRFPQHPLTLPLTKTGEHLDV 226
	*:*. :.* ** * :*:*: **** .

Supplementary Figure 3.

**D. labrax** -----  
*S. maximus* -----MEGFLVSKTVFTSCELGVFDVLLAAECPLSAEEI 34  
*O. niloticus* MADSEKMVPTKVLPTADVYPKRIMEYIEGFLISKTLFTSCELGVFDVLLGSERSLSAEEI 60  
*A. carolinensis* -----MNSTEDLEYLQILIQYQNGFLISKVMFTACELGIFDLLRESKEILSTKTI 50  
*G. gallus* -----MDSTEDLDYPQIIFQYSNGFLVSKVMFTACELGVFDLLQSGRPLSLDVI 50  
*M. mulata* -----MGSSGDDGY-RLLNEYTNGFMVSQVLFACELGVFDLLAEAPGPLDVAAV 49

**D. labrax** -----GQVLYSNTEQASVYLTRSSPVSLYQSVOY 29  
*S. maximus* SQAVGASLDGTERLLAACTGLQLLNTH-QEHGRVLYSNTDEASVYLTRSGPLSLFQSIQY 93  
*O. niloticus* SQAVGASLDGTERLLAACTGMQILNRH-QVDGKVSYSNTEQARLFLTRSSPLSLYQSIHY 119  
*A. carolinensis* AERLGSSIRGMERLLDACVGLKLLRVDKMQEG-AFYGNTEISNLYLTKSGPKSQYHNLMY 109  
*G. gallus* AARLGTSIMGMERLLDACVGLKLLAVELRREG-AFYRNTEISNIYLTSSPKSQYHIMMY 109  
*M. mulata* AAGVEASSHGTELLLDTCVSLKLLKVE-TRAGKAFYQNTLSSAYLTRVSPTSQCNNLLKY 108  
 . \* \*\* : : : \* . : \* \* : : \*

**D. labrax** SSRTIYLCWHYLTDAVREGRNQYEKAFGVSSKDLFQALYRSEEMVKFMQLMNSIWNICG 89  
*S. maximus* SSRTIYFCWHYLTDAVREGRNQYEKAFGVSSKDLFEALYRCEEMVKFMQLMNSIWNICG 153  
*O. niloticus* HSKTIYLCWHYLTDAVREGRNQYEKAFGVSSGDLFEAIYRSDVEEMVKFMQLMHSIWNICG 179  
*A. carolinensis* YSKTIYLCWHYLTDAIREGKNQYERAFGIPSKDVFEALYRSEEMIKFMYGLNATWSICG 169  
*G. gallus* YSNTVYLCWHYLTDAVREGRNQYERAFGISSKDLFGARYRSEEMLKFFLAGQNSIWSICG 169  
*M. mulata* MGRTSYGCWGHLDADVREGKNQYLQTFGVPAEDLFAKAIYRSEGERLQFMQALQEVWSVNG 168  
 . . \* \* \* \* : : \* \* \* \* : : \* \* \* \* : : \* \* \* \* : : \* \* \* \* : : \*

**D. labrax** KDVVTAFDLSPFKVICDLGGCSGALAKQCTSAYPECTVTIFDLPKVVSTBREHFVMEANQ 149  
*S. maximus* KDVVTAFDLSPFKLICDLGGCSGALAKQCTSAYPECTVTIFDLPKVVRMSREHFVGEADL 213  
*O. niloticus* KDVVTAFDLSPFKVICDLGGCSGALAKHCTSAYPECTVTIFDLPKVVHMSKKHFVKEDDQ 239  
*A. carolinensis* RDVLAAFNLSPFVTVIYDLGGGAGALAHCEISLYPNCSVTIFDLPKVVETAKKHVFSSEEQ 229  
*G. gallus* RDVLTAFDLSPFQIYDLGGGGGALAQECVFLYPNCTVTIYDLPKVVQVAKERLVPPEER 229  
*M. mulata* RSVLTAFDLSGFPLMCDLGGGPGALAKECLSLYPGCKVTVFDVPEVVRTAKQHFSPPEE 228  
 : : \* : \* \* \* : : : \* \* \* \* \* \* \* \* : \* \* \* \* \* \* \* \* : : : : :

**D. labrax** RISFHEGDFFKDPLEADLYILAGIHDWTDERSIELLSKVYKACKPGGAVLLVEALIEYE 209  
*S. maximus* RISFHQGDFFKDPLEADLYILARILHDWTDERCIGLIRRIYEACKPGGVLLVEALIEHE 273  
*O. niloticus* RISFHEGDFFKDSLPEAEELYILARILHDWTDERCVELLQRIYKACKPGGAVLLVEALINK 299  
*A. carolinensis* RITFHEGDFFKDPLEADLYILARILHDWADEKCVQLLTKVQKVCCKPGGVLLVETLLNE 289  
*G. gallus* RIAFHEGDFFKDSIPEADLYILSKILHDWDDKCRQLLAEVYKACRPGGVLLVESLLSE 289  
*M. mulata* EIHLQEGDFFKDPLEADLYILARILHDWADGKCSHLLERVYHTCKPGGGILVIESLLDE 288  
 . \* : : \* \* \* \* \* : \* : \* \* \* \* \* : \* : \* \* \* \* \* : . \* \* : . \* : \* \* \* : \* : \* \* :

**D. labrax** DGSGPVTAQLYSLNMLVQTEGRERTAAQYAALLAAAGFRKIQRHLTGKIYDAVLGLKET 268  
*S. maximus* DGSGPLTVQLYSLNMLVQTEGRERTAAQYAALLAAAGFANTQRHLTGKIYDAVLGLKET 332  
*O. niloticus* DGSGPLTTQLYSLNMLVQTEGRERTDVQYAALLTAAGFTNIRHCLTGKIYDAVLGHKKA 358  
*A. carolinensis* DKSGPLESQLYSLNMLVQTEGKERTAAEFTKLLIAAGFLETEIKRTGKLYDAILGRK-- 346  
*G. gallus* DRSGPVETQLYSLNMLVQTEGKERTAVEYSELLGAAGFREVQVRRGTGKLYDAVLGRK-- 346  
*M. mulata* DRRGPLLTQLYSLNMLVQTEGQERTPTHYHMLLSSAGFRDFQFKKGTGAIYDAILVRK-- 345  
 \* \*\* : \* \* \* \* \* \* \* \* \* \* : \* \* : \* \* . . \* \* : \* \* \* : \* \*

Figure 1

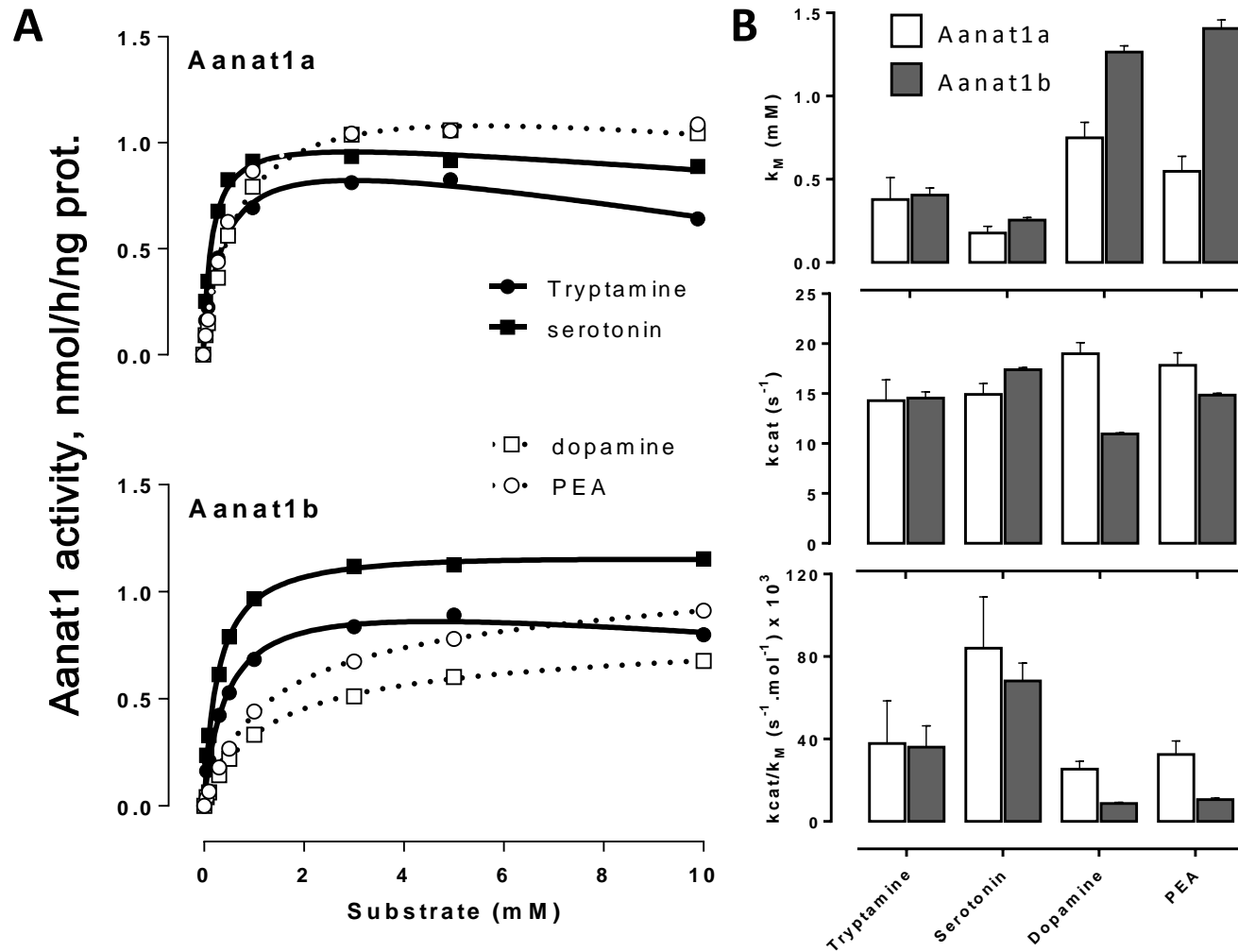
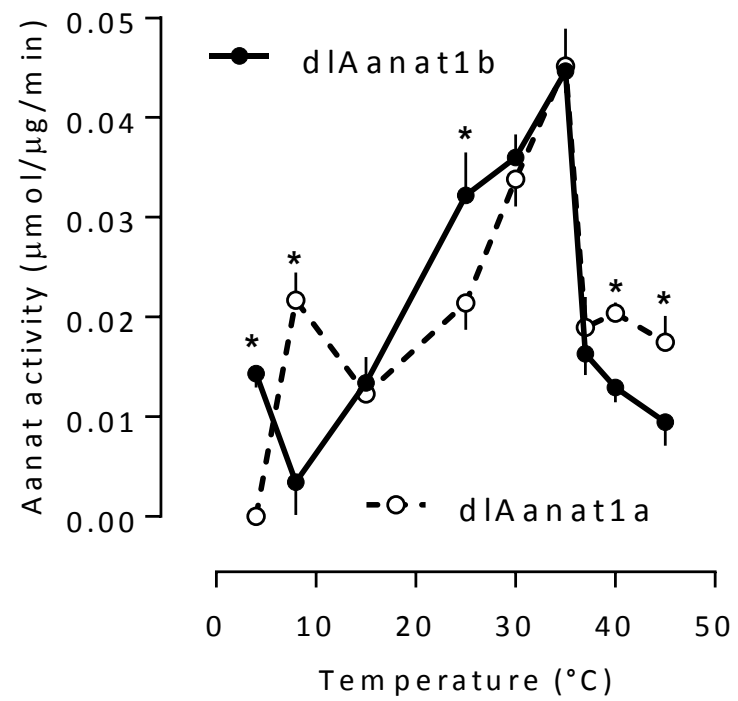
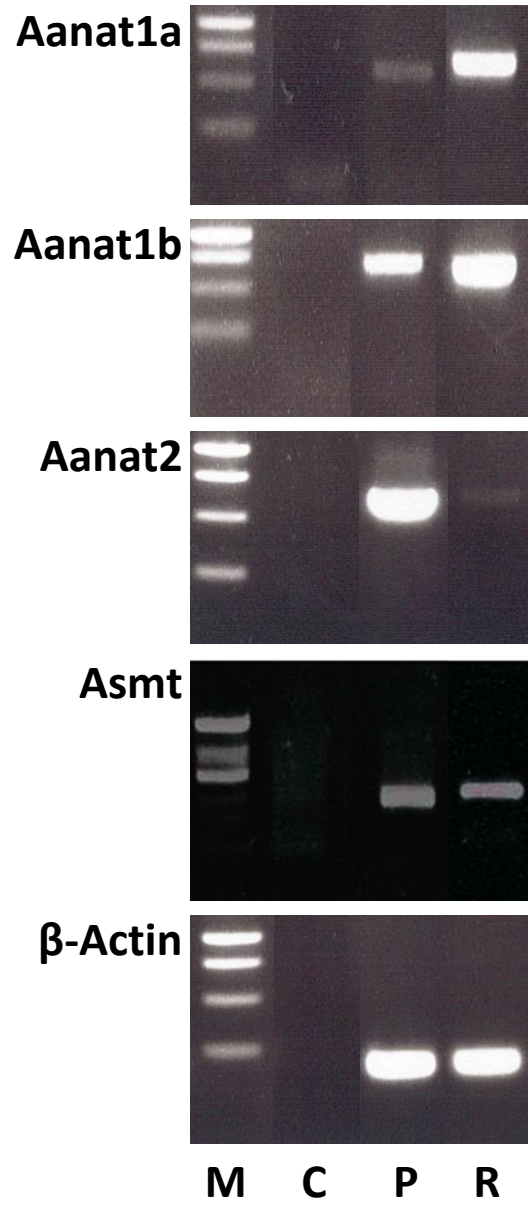


Figure 2





**Figure 4**



**Figure 5**

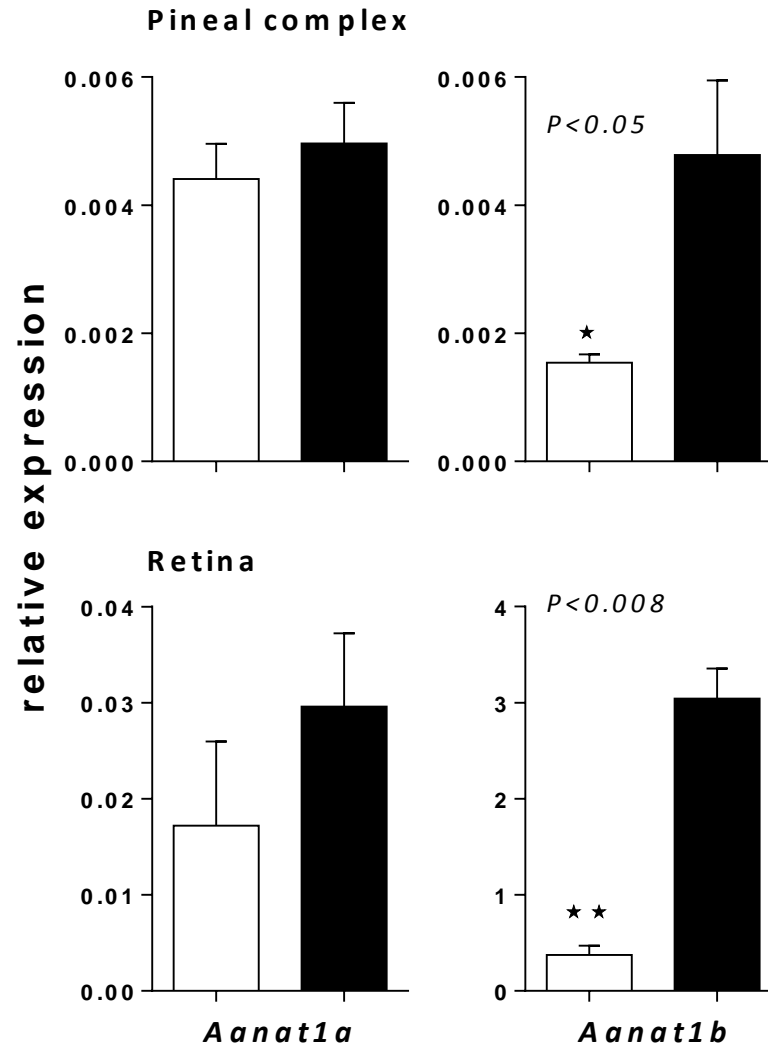


**Figure 6**

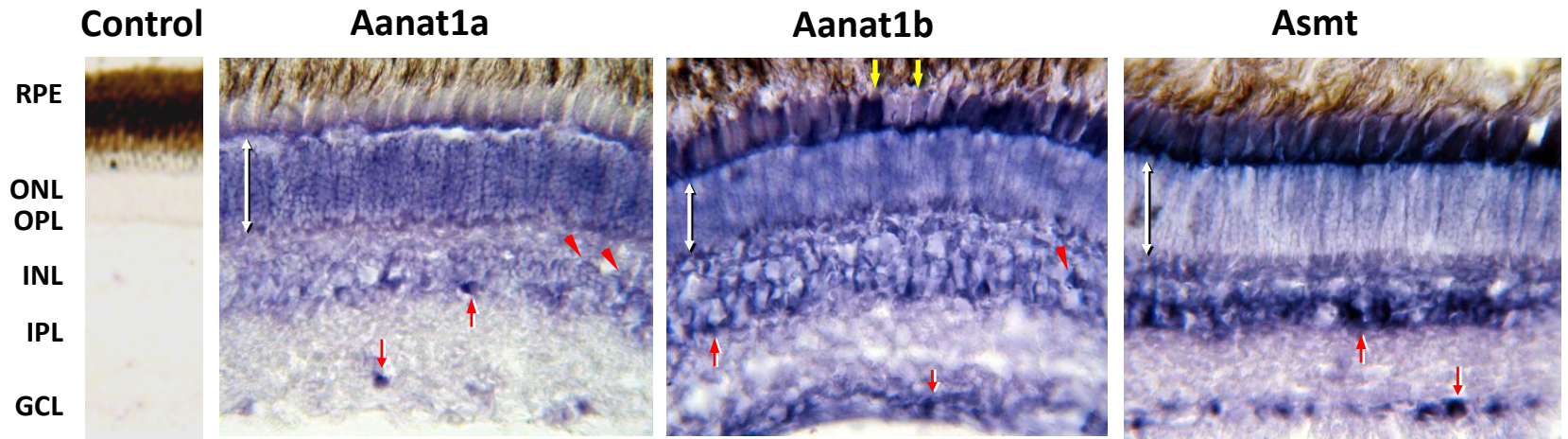


Figure 7

